Conjugated hybrid films based on a new polyoxotitanate monomer

Gang Liu, Xing Yang, Antoine Bonnefont, Yaokang Lv, Jun Chen, Wenyan Dan, Zuofeng Chen, Laurent Ruhlmann, Dominic S. Wright, Cheng Zhang

COMMUNICATION

Novel conjugated hybrid films based on a new polyoxotitanate monomer

Received 00th January 20xx,
Accepted 00th January 20xx

DOI: 10.1039/x0xx00000x

www.rsc.org/

Gang Liu,[a] Xing Yang,[a] Yaokang Lv,[a, d*] Jun Chen,[a] Wenyan Dan,[b] Zuofeng Chen,[b] Laurent Ruhlmann,[d] Dominic S. Wright,[c] Cheng Zhang [a,*]

Novel polyoxotitanate (POT) hexamer [Ti(μ_3-O)(O^{i}Pr)(TA)]$_6$ (TA= thiophene-3-acetic acid) has been employed as a nano-building block, producing a series of novel hybrid conjugated films Poly-(EDOT-POT)s by electrochemical copolymerization with 3,4-ethylenedioxythiophene (EDOT). One of these polymers Poly-(EDOT-POT)-1 can be used as fast-ion electrode material and has improved electrochromic properties and 35% higher capacitance (102.5 F/g) than that of bare PEDOT (75.8 F/g) at a current density of 1 A/g.

Nanostructured titania composites have attracted considerable attention in photocatalysis and photoelectrical applications as well as energy storage due to their inherent physicochemical and unique nanoscale properties.[1-9] However, uneven dispersion, agglomeration and heterogeneous interface problems in their composites often hinder the performances of these material.[10]

During the past decade, there has been considerable interest in polyoxotitanate (**POT**) cages, which possess well-defined inorganic Ti_xO_y cores surrounded by organic ligands.[11-14] Recently, **POT**s have proved to be particular effective precursors for formation of various titania composites, with controlled composition and morphology.[15-21] **POT**s also can be employed as 'nano-blocks' for the formation of new organic-inorganic hybrid materials.[22-27] For example, the introduction of styrenic groups allows copolymerization of the **POT** monomers $Ti_{16}O_{16}(OEt)_{32-x}(OPhCH{=}CH_2)_x$ with styrene to form hybrid materials with three dimensional networks in which the titania nano-fillers are covalently linked to the organic polymer. [25]

[a] College of Chemical Engineering and Materials Science, Zhejiang University of Technology, Hangzhou, 310014, China. E-mail: czhang@zjut.edu.cn, yaokanglv@zjut.edu.cn.

[b] Department of Chemistry, Tongji University, Shanghai 200092, China.

[c] Department of Chemistry, University of Cambridge, Lensfield Road, Cambridge CB2 1EW, UK.

[d] Institut de Chimie (UMR au CNRS n°7177), Université de Strasbourg, 4, rue Blaise Pascal CS 90032, F-67081 Strasbourg Cedex, France.

† Electronic Supplementary Information (ESI) available: Synthesis, crystal data and analytic characterization of **POT-1,** CCDC 1537426; preparation and characterization of **DPE-1**. For ESI and crystallographic data in CIF or other electronic format see DOI: 10.1039/c000000x/.

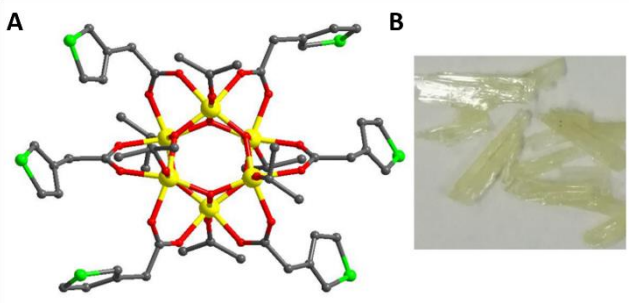

Fig. 1 (A) Solid-state structure of **POT-1**, H-atoms have been omitted for clarity (red = O, gray = C, green = S, yellow = Ti); (B) Photographic image of **POT-1**.

In the current work, we have explored the incorporation of the polymerizable ligand thiophene-3-acetic acid (**TA**) into **POT**s. The new **POT** cage [Ti(μ_3-O)(O^{i}Pr)(TA)]$_6$ (**POT-1**; Fig. 1) functions as a monomer building block in the copolymerization with conjugated monomers such as 3,4-ethylenedioxythiophene (**EDOT**), thiophene or pyrrole, forming a range of hybrid conjugated materials (Scheme 1). The electrochemical performance of these novel materials was studies.

Light yellow crystals of **POT-1** are obtained *via* the solvothermal reaction of Ti(O^{i}Pr)$_4$ and **TA** in propan-2-ol (Fig. 1B and ESI†). A Single crystal X-ray diffraction (sXRD) analysis shows that it has a hexameric 'stack' arrangement with a Ti_6O_6 core (Fig. 1A). Each of the chemically-equivalent Ti(IV) centre has a six-coordinate, octahedral geometry, being bonded to three μ_3-O oxo-atoms within the core, three O atoms from two **TA** ligands and one isopropoxide-O atom. The peripheral "thiophene tentacles" are aligned in opposite directions.

Crystals of **POT-1** are probably stable in air and soluble in various organic solvents like toluene, tetrahydrofuran, chloroform and dichloromethane (DCM). Room-temperature ^{1}H NMR spectrum of **POT-1** in $CDCl_3$ shows one doublet corresponding to the methyl-H at 1.2-1.3 ppm and one septet associated to -CH near 4.8-5.0 ppm which represent the ^{i}PrO ligands (Fig. S1). The three signals at 7.20, 7.11, and 6.98 ppm with the relative intensity is near 1:1:1 as well as the singlet at 3.55 ppm are belong to the characteristic peaks of thiophene-3-acetic acid. The peak area ratios in ^{1}H NMR indicate that the ratio of the **TA** to ^{i}PrO ligands in **POT-1** is 1:1 (Fig. S1). Interestingly, the NMR spectrum for **POT-1** is not obviously changed

with concentration, which suggests that the structure remains the same in $CDCl_3$.

As shown in Fig. S3, The +ve ion electrospray mass spectrum shows a signal at m/z = 1586.87 for $[M+H]^+$ (calc. 1585.92). The bulk purity of crystalline **POT-1** is confirmed by the powder X-ray diffraction (pXRD) spectrum which is identical to the pattern derived from its sXRD data (Fig. S2). Thermogravimetric (TGA) and differential thermal analysis (DTA) show that **POT-1** is not thermally decomposed at temperatures lower than 150°C (Fig. S4). Comparable with reported **POT** cages, the band gap determined from the solution-state UV visible spectrum of **POT-1** is ca. 3.79 eV (Fig. S5). [28]

POT-1 is the first structurally determined **POT** cage in which the assembly is achieved exclusively by incorporation of polymerizable **TA** ligand into a Ti_xO_y core.

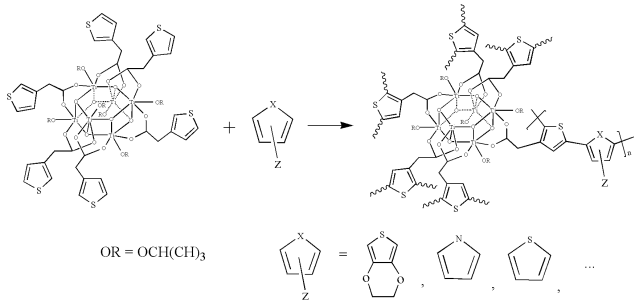

Scheme 1 copolymerization strategy used to obtain conjugated hybrid materials from **POT-1**.

Cyclic voltammetry (CV) curves of **POT-1** in a DCM solution of 0.1 M tetrabutylammonium hexafluorophosphate (TBAH) exhibit an irreversible multistage oxidation process with initial oxidation potential at 1.05 V, very close to that of **EDOT** (Fig. S7). The similarity of the initial oxidation potentials was propitious for the controllable formation of the copolymers.[29-30.] Subsequently, a series of conjugated hybrid films **Poly-(EDOT-POT)s** was produced by electrochemical copolymerization of POT-1 with **EDOT** indium-doped tin oxide (ITO) glass substrates by a potentiostatic method (See ESI†) (Scheme 1).

As shown in Fig. 2, a series of **Poly-(EDOT-POT)s** with various morphologies were prepared through potentiostatic copolymerization of POT-1 and EDOT with a 1:1 molar ratio at different anodic potentials. It is noteworthy that a 3D nanoporous film named **Poly-(EDOT-POT)-1** was obtained at 1.7V. To the best of our knowledge, this phenomenon was observed for the first time, and may be due to the multiple polymerizable sites and multistage oxidation processes of **POT-1** that can lead to various polymer networks under different electrochemical conditions. As shown in Fig. S8, the morphology of **Poly-(EDOT-POT)s** films can also be altered significantly by adjusting the proportion of **POT-1** and **EDOT** co-monomers.

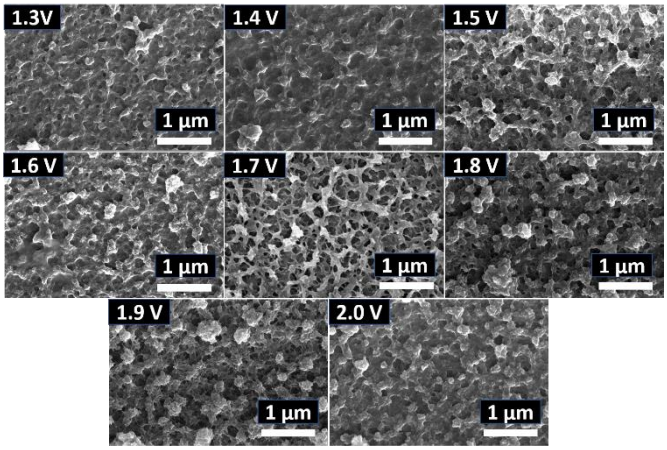

Fig. 2 SEM images of Poly-(EDOT-POT)s films on ITO electrodes through potentiostatic copolymerization of POT-1 and EDOT (1:1 molar ratio) on ITO at 1.3V, 1.4V, 1.5V, 1.6V, 1.7V, 1.8V, 1.9V and 2.0 V respectively.

Energy dispersive spectroscopy (EDS) suggests that **Poly-(EDOT-POT)-1** contains 2.05% atom% Ti atoms (Fig. S14, Table S3), and element mapping indicates that Ti is disperse homogeneously in the matrix (Fig. 3). **Poly-(EDOT-POT)-1** is a stable film where the dispersion of Ti in **Poly-(EDOT-POT)-1** was not changed after soaked in DCM even during 2 weeks (Fig. S18).

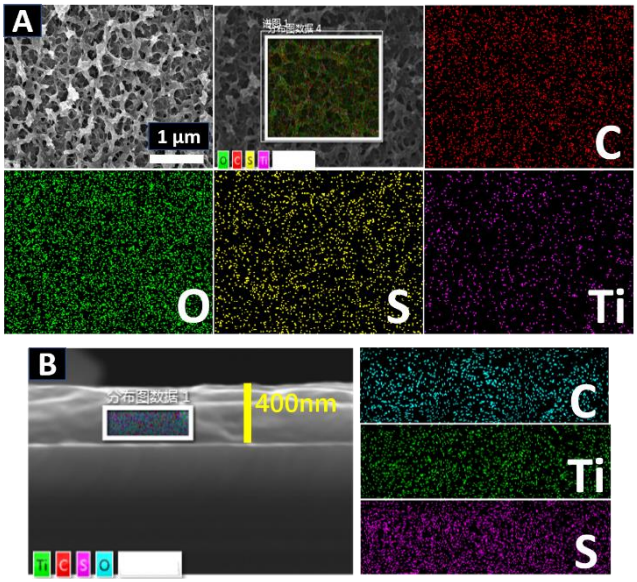

Fig. 3 SEM and element mapping of plane (A) and section (B) of the **Poly-(EDOT-POT)-1** film.

CV curves of **Poly-(EDOT-POT)-1** and **PEDOT** films on a glassy carbon electrode were tested in a three-electrode system with Ag/AgCl as reference electrode. As shown in Fig. S19, **PEDOT** film exhibits a redox pair (E_{pc}= -0.59V, E_{pa}= 0.09V) in the potential range from -0.8 to 1.5 V, while there is only one significant reduction peak around 0.20 V for the film of **Poly-(EDOT-POT)-1** at scan rate of 10 mV/s.

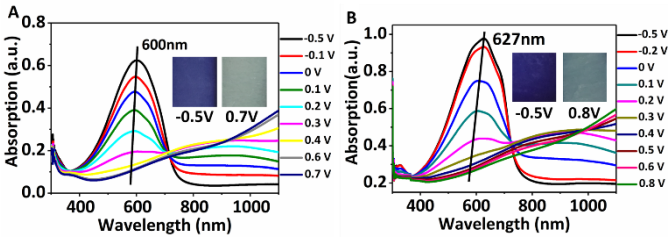

Fig. 4 UV–vis spectra of (A) **Poly-(EDOT-POT)-1** and (B) **PEDOT** at applied voltages between -0.8 V and 1.2 V in 0.1 M TBAH/DCM solution (inset are the photographs of the corresponding polymer films on ITO glass).

Visible and NIR transmission spectra of **Poly-(EDOT-POT)-1** and **PEDOT** on ITO at different potentials are shown in Fig. 4. Like **PEDOT**, **Poly-(EDOT-POT)-1** is a cathodically-colouring material with the colour changed from dark blue (coloured state) at −0.5 V to light-blue (bleached state) at 0.7 V. In the coloured state, the visible absorption band of **Poly-(EDOT-POT)-1** (600 nm) is blue shifted compare with that of **PEDOT** (627 nm), which may be due to the attachment of **POT-1** to the conjugated backbone. As shown in Fig. 5, **Poly-(EDOT-POT)-1** exhibits improved electrochromic properties with larger optical contrast (53.0%) and shorter coloring time (1.36 s) compare with that of **PEDOT** (50.7% optical contrast, 1.59s coloring time), which may be due to the nanoporous structure of **Poly-(EDOT-POT)-1**.

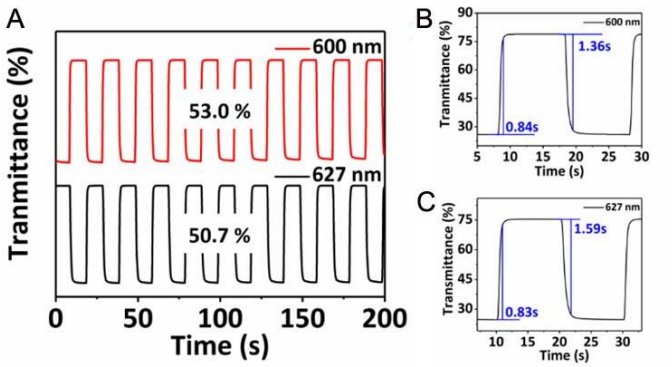

Fig. 5 Optical contrast of the **Poly-(EDOT-POT)-1** (red curve) polymer films monitored between -0.5 V and 0.7 V and the **PEDOT** (black curve) films monitored between -0.5 V and 0.8 V in 0.1 M TBAH/DCM solution with a residence of 10 s (A); Electrochromic switching response of **Poly-(EDOT-POT)-1** (B) and **PEDOT** (C).

As an electrode material for supercapacitor **Poly-(EDOT-POT)-1** was further tested in a three-electrode system using 0.1 M $LiClO_4$/ACN as the electrolyte (ESI†). Nyquist plots of **Poly-(EDOT-POT)-1** and **PEDOT** are shown in Fig. S20. It can be seen that the internal resistance of **Poly-(EDOT-POT)-1** is smaller than that of **PEDOT**, which suggests that the **Poly-(EDOT-POT)-1** electrode has better conductive properties[31] and consequent electrochemical properties.

CV curves of **Poly-(EDOT-POT)-1** and **PEDOT** both exhibit a quasi-rectangular shape at sweep rates from 10 to 300 mV/s, but the specific capacitance of **Poly-(EDOT-POT)-1** is larger than that of **PEDOT** especially at higher scanning rate (Fig.6A, 6B); charge-discharge curves at current densities between 1A/g and 5 A/g display regular-triangular shapes and no obvious voltage drop can be observed at the beginning of the discharge process for both the **Poly-(EDOT-POT)-1** and **PEDOT** electrodes indicating ideal capacitor behaviour (Fig.6C, 6D). It is noteworthy that the specific capacitance of **Poly-(EDOT-POT)-1** is 102.5 F/g at a current density of 1 A/g much higher than that of bare **PEDOT** (75.8 F/g). With the increase of current densities to 5 A/g, the specific capacitance of **Poly-(EDOT-POT)-1** decreases to 94.1 F/g , 34% higher than that of **PEDOT** which is 70.3 F/g (Fig. 6E). As shown in Fig. 6F, **Poly-(EDOT-POT)-1** delivered a higher energy density of 14.2 Wh/kg at power density of 500 W/kg and a higher power density of 2500 W/kg at energy density of 13.1 Wh/kg compare with that of **PEDOT**. These results indicate that **Poly-(EDOT-POT)-1** is a promising electrode material suitable for fast ion transport. [32]

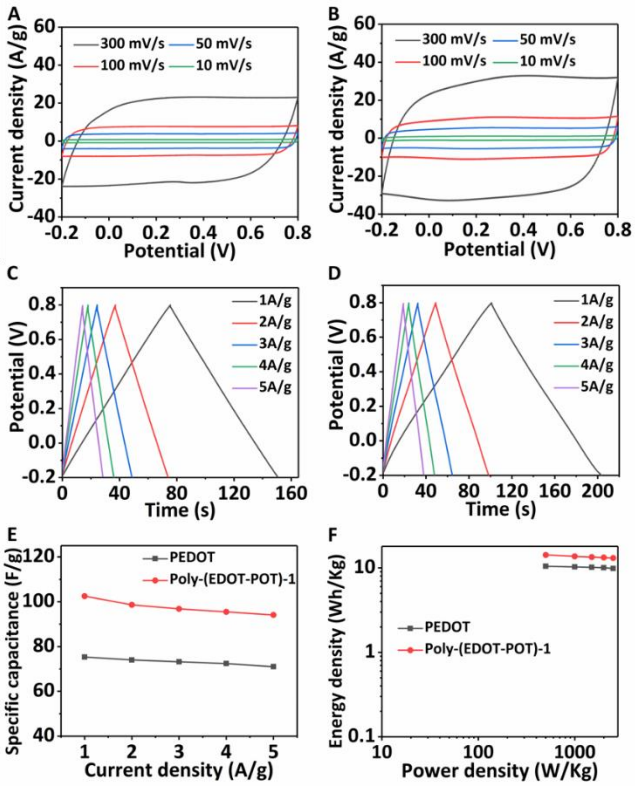

Fig. 6 CV curves of **PEDOT** (A) and **Poly-(EDOT-POT)-1** (B); galvanostatic charge/discharge curves of **PEDOT** (C) and **Poly-(EDOT-POT)-1** (D); specific capacitance calculated from discharge curves of **PEDOT** and **Poly-(EDOT-POT)-1** (E); Ragone plots of **PEDOT** and **Poly-(EDOT-POT)-1** (F).

Conclusions

In summary, **POT-1** is the first structurally determined **POT** cage in which the assembly is achieved exclusively by incorporation of polymerizable **TA** ligand into a Ti_xO_y core. A series of conjugated hybrid films **Poly-(EDOT-POT)s** has been synthesized employing the **POT-1** as a nanobuilding block. 3D nanoporous film **Poly-(EDOT-POT)-1** is a promising electrode material suitable for fast ion transport and exhibit improved electrochromic properties and 35% higher capacitance (102.5 F/g) compared with that of **PEDOT** (75.8 F/g) at a current density of 1 A/g.

Conflicts of interest

There are no conflicts to declare.

Acknowledgements

We sincerely thank National Natural Science Foundation of China (NSFC, No. 21501148).

Notes and references

1 L. Lin, H. Wang and P. Xu, *Chem. Eng. J.*, 2017, **310**, 389-398.

2 N. Singh, Z. Salam, A. Subasri, N. Sivasankar and A. Subramania, *Sol. Energy Mater. Sol. Cells*, 2018, **179**, 417-426.

3 D. Zheng, Y. Xin, D. Ma, X. Wang, J. Wu and M. Gao, *Catal. Sci. Technol, 2016, **6**, 1892-1902.*

4 *B. Li, B. Xi*, Z. Fen**g,** Y. Lin, J. Liu, J. Feng, Y. Qian and S. Xiong, *Adv. Mater.*, 2018, ***30**, 1705788.*

5 *J.* Wang, W**.** Liu, H. Li, H. Wang, Z. Wang, W. Zhou and H. Liu, Chem. Eng. J., 2013, **228**, 272-280.

6 J. Liu, Z. Cai, Y. Lv, Y. Zhang, C. Su, M. Ouyang, C. Zhang and D. S. Wright, *J. Mater. Chem. A*, 2015, **3**, 1837-1840.

7 J. Ma, W. Liu, X. Liang, B. Quan, Y. Cheng, G. Ji and W. Meng, *J. Alloys Compd.*, 2017, **728**, 138-144.

8 T. D. Savić, Z. V. Šaponjić, M. I. Čomor, J. M. Nedeljković, M. D. Dramićanin, M. G. Nikolić, D. Ž. Veljković, S. D. Zarić and I. A. Janković, *Nanoscale*, 2013, **5**, 7601-7612.

9 M.-B. Alexandra, L.-C. María, F.-G. Marta, K. Anna, F. Manuel and F.-G. Marcos, *Int. J. Mol. Sci.*, 2013, **14**, 9249-9266.

10 (a) M. Ihalainen, T. Lind, T. Torvela, K. E. J. Lehtinen and J. Jokiniemi, *Aerosol Sci. Technol*, 2012, **46**, 990-1001; (b) B. Luo, Y. Deng, Y. Wang, Z. Zhang and M. Tan, *J. Alloys Compounds*, 2012, **517**, 192-197; (c) X. Hua, F. L. Bei, and X. Wang, *J. Appl. Polym. Sci.*, 2009, **112**, 3582–3588.

11 C. Zhao, Y.-Zi. Han, S. Dai, X. Chen, J. Yan, W. Zhang, H. Su, S. Lin, Z. Tang, B. K. Teo and N. Zheng, *Angew. Chem., Int. Ed.*, 2017, **56**, 16252 –16256.

12 H. Assi, G. Mouchaham, N. Steunou, T. Devic and C. Serre, *Chem. Soc. Rev.*, 2017, **46**, 3431-3452.

13 G. Zhang, C. Liu, D.-L. Long, L. Cronin, C.-H. Tung and Y. Wang, *J. Am. Chem. Soc*., 2016, **138**, 11097-11100.

14 P. I. Molina, K. Kozma, M. Santala, C. Falaise and M. Nyman, *Angew. Chem., Int. Ed.*, 2017, **56**, 16277 –16281.

15 Y. Lv, Z. Cai, D. Yan, C. Su, W. Li, W, Chen, Z. Ren, Y. Wei, O. Mi, C. Zhang and D. S. Wright, *RSC Adv.*, 2016, **6**, 57–60.

16 Y. Lv, W. Du, Y. Ren, Z. Cai, K. Yu, C. Zhang, Z. Chen and D. S. Wright, *Inorg. Chem. Front.*, 2016, **3**, 1119–1123.

17 Y. Fan, H.-M. Li, R.-H. Duan, H.-T. Lu, J.-T. Cao, G.-D. Zou and Q.-S. Jing, *Inorg. Chem.*, 2017, **56**, 12775-12782.

18 P. Ji, Y. Song, T. Drake, S. S. Veroneau, Z. Lin, X. Pan and W. Lin, *J. Am. Chem. Soc.*, 2018, **140**, 433-440.

19 G. Zhang, W. Li, C. Liu, J. Jia, C.-H. Tung and Y. Wang, *J. Am. Chem. Soc*., 2018, **140**, 66-69.

20 F. G. Svensson, G. A. Seisenbaeva and Va. G. Kessler, *Eur. J. Inorg. Chem.*, **2017**, 35, 4117–4122.

21 W. H. Fang, L. Zhang and J. Zhang, *Chem. Commun.*, 2017, **53**, 3949—3951.

22 L. Rozes and C. Sanchez, *Chem. Soc. Rev.*, 2011, **40**, 1006–1030.

23 C. Sanchez, C. Boissiere, S. Cassaignon, C. Chaneac, O. Durupthy, M. Faustini, D. Grosso, C. Laberty-Robert, L. Nicole, D. Portehault, F. Ribot, L. Rozes and C. Sassoye, *Chem. Mater.*, 2014, **26**, 221−238.

24 G. L. Drisko and C. Sanchez, *Eur. J. Inorg. Chem.*, 2012, **32**, 5097–5105.

25 L. Rozes, G. Fornasieri, S. Trabelsi, C. Creton, N. E. Zafeiropoulos, M. Stamm and C. Sanchez, *Prog. Solid State Chem.*, 2005, **33**, 127-135.

26 S. Trabelsi, A. Janke, R. Hässler, N. E. Zafeiropoulos, G. Fornasieri, S. Bocchini, L. Rozes, M. Stamm, J.-F. Gérard and C. Sanchez, *Macromolecule*, 2005, **38**, 6068-6078.

27 F. Périneau, S. Pensec, C. Sassoye, F. Ribot, L. Lokeren, R. Willem, L. Bouteiller, C. Sanchez and L. Rozes, *J. Mater. Chem.*, 2011, **21**, 4470–4475.

28 (a) Y. Chen, J. Sokolow, E. Trzop, Y.-S. Chen and P. Coppens, *J. Chin. Chem. Soc.*, 2013, **60**, 887; (b) Y. Lv, J. Cheng,P. D. Matthews, J. P. Holgado, J. Willkomm, M. Leskes,A. Steiner, D. Fenske, T. C. King, P. T. Wood, L. Gan, R. M. Lambert and D. S. Wright, *Dalton Trans.*, 2014, **43**, 8679–8689; (c) Y. Chen, E. Trzop, A. Makal, Y.-S. Chen and P. Coppens, *Dalton Trans.*, 2014, **43**, 3839.

29 C. L. Gaupp and J. R. Reynolds, *Macromolecules*, 2003, **36**, 6305-6315.

30 (a) C. Zhang, C. Hua, G. Wang, M. Ouyang and C. Ma, *Electrochim. Acta*, 2010, **55**, 4103-4111. (b) Yaokang L, Liu Y, Yun P, et al. Preparation,Characterisation and Electrochromic Properties of Copolymer Films Based on 3,4-Ethylenedioxythiophene and Pyrrole-3-Carboxylic Acid · [J]. Chemical Journal of Chinese Universities, 2017.

31 X. Xu, W. Shi, P. Li, S. Ye, C. Ye, H. Ye, T. Lu, A. Zheng, J. Zhu, L. Xu, M. Zhong and X. Cao, Chem. Mater., 2017, **29**, 6058-5065.

32 (a) Z. Xu, J. Wang, Z. Hu, R. Geng and L. Gan, *Electrochim. Acta*, 2017, **231**, 601-608. (b) W. Du, Y. Lv, Z. Cai, C. Zhang, Acta Phys. Chim. Sin. 33 (9) (2017) 1828–1837.